Instability and Pattern Formation in Thin Liquid Films on Chemically Heterogeneous Substrates

ARTICLE *in* LANGMUIR · NOVEMBER 2000

Impact Factor: 4.46 · DOI: 10.1021/la000759o

3 AUTHORS, INCLUDING:

Kajari Kargupta
Jadavpur University
60 PUBLICATIONS **1,323** CITATIONS
SEE PROFILE

Ashutosh Sharma IITK
Indian Institute of Technology Kanpur
328 PUBLICATIONS **7,324** CITATIONS
SEE PROFILE

Instability and Pattern Formation in Thin Liquid Films on Chemically Heterogeneous Substrates

Kajari Kargupta, Rahul Konnur, and Ashutosh Sharma*

Department of Chemical Engineering, Indian Institute of Technology at Kanpur, Kanpur 208016, India

Received May 31, 2000. In Final Form: September 6, 2000

The surface instability, dynamics, morphology, and spontaneous dewetting of a thin liquid film on chemically heterogeneous substrates are studied on the basis of 3D nonlinear simulations. A new mechanism of dewetting in the presence of heterogeneity is proposed where the instability is engendered by the gradient of intermolecular interactions that lead to a microscale wettability contrast. The time scale of instability, which can be several orders smaller than the spinodal dewetting time scale on homogeneous surfaces, varies inversely with the potential difference induced by the heterogeneity. Heterogeneity can even destabilize spinodally stable films, reduce the time of rupture substantially for thicker films, and decrease the dependence of rupture time on the film thickness. The presence of heterogeneity produces complex and locally ordered morphological features that are not predicted by the spinodal dewetting, for example "ripples" and "castle-moat" structures, radially symmetric structures, and a lack of undulations before the birth of a hole. The precise morphological pattern selection depends on the size of the heterogeneity, the potential difference caused by the heterogeneity, the film thickness, and also the spinodal characteristics of the substrate. The resulting morphologies can be understood on the basis of simple arguments that consider interplay among these factors.

1. Introduction

The stability and the wetting behavior of thin (<100 nm) liquid (e.g., polymer) films on a solid substrate[1−28] are of technological and scientific importance in applications ranging from coatings, paints, dielectric layers, thin film lubrication, and microelectronic and optoelectronic devices to fundamental studies of multilayer adsorption and polymer diffusion. Most of the naturally occurring surfaces as well as variously tailored substrates used in thin film experiments are chemically heterogeneous on nanometer to micrometer scales, for example, due to contamination, cavities, an uneven oxide layer, and so forth. Deliberately tailored chemically heterogeneous substrates are also increasingly being used for engineering of desired nano- and micropatterns in thin films.[18,19,29−41]

We have recently proposed a new mechanism of instability of thin films on heterogeneous surfaces,[26] where the surface instability leading to dewetting is derived from the *gradient* of wettability rather than from the nonwettability of the substrate itself as in the spinodal dewetting. A more comprehensive account of the spatiotemporal evolution of the instability, its dynamics and morphology, and its length and time scales is considered here.

The current theoretical understanding of the thin film stability, dynamics, and morphology is limited to films on chemically homogeneous substrates. Such films are

* To whom correspondence should be addressed. E-mail: ashutos@iitk.ac.in. Fax: (91) 512 590104.

(1) Reiter, G.; Sharma, A.; Casoli, A.; David, M.; Khanna, R.; Auroy, P. *Langmuir* **1999**, *15*, 2551.
(2) Kim, H. I.; Mate, C. M.; Hannibal, K. A.; Perry, S. S. *Phys. Rev. Lett.* **1999**, *82*, 3496.
(3) Sferrazza, M.; Heppenstall-Butler, M.; Cubitt, R.; Bucknall, D.; Webster, J.; Jones, R. A. L. *Phys. Rev. Lett.* **1998**, *81*, 5173.
(4) Sharma, A.; Khanna, R. *Phys. Rev. Lett.* **1998**, *81*, 3463.
(5) Sharma, A.; Khanna, R. *J. Chem. Phys.* **1999**, *110*, 4929.
(6) Xie, R.; Karim, A.; Douglas, J. F.; Han, C. C.; Weiss, R. A. *Phys. Rev. Lett.* **1998**, *81*, 1251.
(7) Herminghaus, S.; Jacobs, K.; Mecke, K.; Bischof, J.; Fery, A.; Ibn-Elhaj, M.; Schlagowski, S. *Science* **1998**, *282*, 916.
(8) Jacobs, K.; Herminghaus, S.; Mecke, K. R. *Langmuir* **1998**, *14*, 965.
(9) Thiele, U.; Mertig, M.; Pompe, W. *Phys. Rev. Lett.* **1998**, *80*, 2869.
(10) Stange, T. G.; Evans, D. F.; Hendrickson, W. A. *Langmuir* **1997**, *13*, 4459.
(11) Kressler, J.; Wang, C.; Kammer, H. W. *Langmuir* **1997**, *13*, 4407.
(12) Bischof, J.; Scherer, D.; Herminghaus, S.; Leiderer, P. *Phys. Rev. Lett.* **1996**, *77*, 1536.
(13) Elbaum, M.; Lipson, S. *Phys. Rev. Lett.* **1994**, *72*, 3562.
(14) Guerra, J. M.; Srinivasrao, M.; Stein, R. S. *Science* **1993**, *262*, 1395.
(15) Zhao, W.; Rafailovich, M. H.; Sokolov, J. *Phys. Rev. Lett.* **1993**, *70*, 1453.
(16) Reiter, G. *Phys. Rev. Lett.* **1992**, *68*, 75.
(17) Reiter, G. *Langmuir* **1993**, *9*, 1344.
(18) Gau, H.; Herminghaus, S.; Lenz, P.; Lipowsky, R. *Science* **1999**, *283*, 46.
(19) Lenz, P.; Lipowski, R. *Phys. Rev. Lett.* **1998**, *80*, 1920.
(20) Sharma, A. *Langmuir* **1993**, *9*, 861.
(21) Sharma, A.; Jameel, A. T. *J. Colloid Interface Sci.* **1993**, *161*, 190.
(22) van der Wielen, M. W. J.; Cohen Stuart, M. A.; Fleer, G. J. *Langmuir* **1998**, *14*, 7065.
(23) Sharma, A.; Reiter, G. *J. Colloid Interface Sci.* **1996**, *178*, 383.
(24) Khanna, R.; Jameel, A. T.; Sharma, A. *Ind. Eng. Chem. Res.* **1996**, *35*, 3081.
(25) Ghatak, A.; Khanna, R.; Sharma, A. *J. Colloid Interface Sci.* **1999**, *212*, 483.
(26) Konnur, R.; Kargupta, K.; Sharma, A. *Phys. Rev. Lett.* **2000**, *84*, 931.
(27) Reiter, G.; Auroy, P.; Auvray, L. *Macromolecules* **1996**, *29*, 2150.
(28) Sharma, A.; Khanna, R.; Reiter, G. *Colloids Surf., B: Biointerfaces* **1999**, *14*, 223.
(29) Rockford, L.; Liu, Y.; Mansky, P.; Russell, T. P. *Phys. Rev. Lett.* **1999**, *82*, 2602.
(30) Paterson, A.; Fermigier, M. *Phys. Fluids* **1997**, *9*, 2210.
(31) Bauer, C.; Dietrich, S. *Phys. Rev. E* **1999**, *60*, 6919.
(32) Pompe, T.; Frey, A.; Herminghaus, S. *Langmuir* **1998**, *14*, 2585.
(33) Gleiche, M.; Chi, L. F.; Fuchs, H. *Nature* **2000**, *403*, 173.
(34) Kataoka, D. E.; Troian, S. M. *Nature* **1999**, *402*, 794.
(35) Lenz, P.; Lipowsky, R. *Eur. Phys. J. E* **2000**, *1*, 249.
(36) Kumar, A.; Whitesides, M. *Science* **1994**, *263*, 60.
(37) Nisato, G.; Ermi, B. D.; Douglas, J. F.; Karim, A. *Macromolecules* **1999**, *32*, 2356.
(38) Karim, A.; Douglas, J. F.; Lee, B. P.; Glotzer, S. C.; Rogers, J. A.; Jackman, R. J.; Amis, E. J.; Whitesides, G. M. *Phys. Rev. E* **1998**, *57*, R6273.
(39) Kielhorn, L.; Muthukumar, M. *J. Chem. Phys.* **1999**, *111*, 2259.
(40) Chou, S. Y.; Zhuang, L.; Guo, L. *Appl. Phys. Lett.* **1999**, *75*, 1004.
(41) Boltau, M.; Walhelm, S.; Mlynek, J.; Krausch, G.; Steiner, U. *Nature* **1998**, *391*, 877.

10.1021/la000759o CCC: $19.00
Published on Web 11/21/2000

rendered unstable by a spinodal mechanism, for which it is necessary that the second derivative of the excess intermolecular interaction energy with respect to the film thickness should be negative. The spinodal evolution is characterized by the appearance of strongly correlated undulations of gradually increasing amplitude on the free surface of the film. Growth of surface instability leads to roughening of the film by creation of thinner and thicker regions. Dewetting eventually occurs by the formation of circular holes or by the formation of bicontinuous undulations/droplets for relatively thick and thin film, respectively. The characteristic length scale of the instability, $\lambda_m \propto h^2$, and the time of rupture, $t_r \propto h_0^5$, if the instability is caused by the nonretarded van der Waals interactions.[4,5,20,21,23,24]

Thus far, only a handful of experiments have hinted at the possibility of witnessing the spinodal dewetting in its pristine form, but a majority have displayed a variety of deviations from the expected behavior. Most important among these are observations of the film remaining flat away from the point at which the rupture first occurs,[7,10] the absence of surface undulations preceding rupture of the film,[7,8,10,12] widely differing morphologies on different parts of the substrate, a wide discrepancy between the predicted and the observed rupture times for thick films,[7,8,12] rupture of spinodally stable films, and complex localized morphologies which are not predicted by simulations on a homogeneous substrate.[1,7,11,14,15] Interesting among these complex morphologies are the laterally layered structures[14] and the presence of mixed morphologies, for example, the coexistence of holes, drops, and undulations.[7] These observations have repeatedly suggested the involvement of heterogeneous sites, for example dust, trapped microcavities, chemical contamination, variation of the oxide layer thickness on silicon, variable chain adsorption, and so forth, all of which generate localized patches of surface properties or potential different from that of the surrounding bulk of the substrate. The objective of this paper is to propose and study a new mechanism of thin film instability on chemically heterogeneous substrates. In particular, effects of chemical heterogeneity on the length scale, time scale, and pattern formation are studied on the basis of direct 3D nonlinear simulations. The general dynamical and morphological features of instability are then clearly contrasted with the spinodal dewetting.

2. Theory

2.1. Thin Film Equation. We consider a thin (<100 nm) Newtonian fluid film on a solid surface ($x-y$ plane). The following "long wave" equation describes the 2D dynamics and the resulting 3D shape, $h = h(x,y,t)$, of a thin film,[4,5,21,23−26]

$$3\mu\, \partial h/\partial t + \nabla\cdot[\gamma h^3 \nabla(\nabla^2 h)] - \nabla\cdot[h^3\, \nabla\phi] = 0 \qquad (1)$$

where $h(x,y,t)$ is the local film thickness, the plane $x-y$ coincides with the substrate, μ and γ are the film viscosity and the surface tension of the film, and $\phi = (\partial \Delta G/\partial h)$ is the conjoining pressure of the film due to excess intermolecular interactions. Equation 1 is the sum of three forces, which are unsteady force/pseudoviscous force (first term), surface tension force due to local curvature of the free surface (second term), and the sum of excess intermolecular forces (third term). The unsteady force, which includes viscous effects, merely retards the growth of instability. The surface tension effect in a 3D geometry may be stabilizing (due to "in-plane curvature as in 2D geometry") or destabilizing (due to "transverse curvature as in Rayleigh instability of circular cylinders"). Finally, a gradient of conjoining pressure causes flow of fluid in the direction of decreasing force per unit area, ϕ. For homogeneous substrates, $\phi = \phi(h)$, and the interfacial instability is caused by flow from thinner to thicker regions only when $\partial\phi/\partial h < 0$ (negative "diffusivity"). Linear stability analysis of eq 1 provides the following spinodal dominant length and time scales for the growth of instability[4,5,21,23−26]

$$\lambda_m = (-8\pi^2\gamma/(\partial^2\Delta G/\partial h^2))^{1/2}; \quad t_r \sim 12\mu\gamma/h^3(\partial^2\Delta G/\partial h^2)^2$$

The neutral wavelength is given by $\lambda_c = (-4\pi^2\gamma/(\partial^2\Delta G/\partial h^2))^{1/2}$. Only the modes with length scales larger than λ_c can amplify.

An extensive set of nonlinear 2D and 3D simulations have verified the above and established the following hallmarks of the spinodal dewetting: (a) initially, a strongly correlated, small amplitude undulating pattern emerges which grows exponentially at small times; (b) dewetting eventually occurs by the formation of circular holes or by the formation of bicontinuous undulations/droplets for relatively thick and thin films, respectively. The characteristics of a pattern and its pathway of evolution thus depend crucially on the form of the intermolecular potential in an extended neighborhood of the initial thickness.[4,5]

However, on a chemically heterogeneous substrate, $\phi = \phi(h,x,y)$, and thus, another mode of surface instability driven by the spatial gradient of force, $\nabla\phi$, is also present even at *constant* film thickness. This microscale wettability contrast causes flow from the less wettable (higher pressure) to more wettable (low-pressure) regions, even when the spinodal stability condition $\partial\phi/\partial h > 0$ is satisfied everywhere.[26]

To assess the role of nonlinearities, linearization of eq 1 around the mean thickness $h = h_0$, using $h(x,y,t) = h_0 + f(x,y,t)$, with $f \ll h_0$, gives the following nonhomogeneous equation.

$$3\mu\, \partial f/\partial t + \gamma h_0^3 \nabla^4 f - h_0^3\, \partial\phi/\partial h|_{h=h_0} \nabla^2 f = h_0^3 \nabla^2 \phi|_{h=h_0} \qquad (2)$$

The nonhomogeneous term, $\nabla^2\phi|_{h=h_0}$, leads to local instability by engendering flow from less wettable to more wettable regions. The mechanism is analogous to the Marangoni flow, except that it derives from the gradient of the excess intermolecular free energy rather than from the variation of surface tension at the free film surface. The same phenomenon is responsible for climbing of a macroscopic drop on a substrate with a wettability gradient.[42] We have modeled the effect of chemical heterogeneity by imposing a step change in ϕ on two different parts of the substrate. The local depression of film thickness resulting from this flow due to the wettability gradient accelerates the overall dewetting process when the film thickness is in the spinodally unstable region. For spinodally stable films, positive values of $\partial\phi/\partial h|_{h=h_0}$ tend to stabilize the film. However, when the flow engendered by wettability gradient is sufficient to lower the local film thickness below a critical thickness where the film becomes spinodally unstable, both mechanisms conspire to produce an explosive rupture.

2.2. Excess Intermolecular Interactions. For simulations, we have considered a fairly general class of excess intermolecular interaction free energy characterized by

(42) Chaudhuri, M. K.; Whitesides, G. M. *Science* **1992**, *256*, 1539.

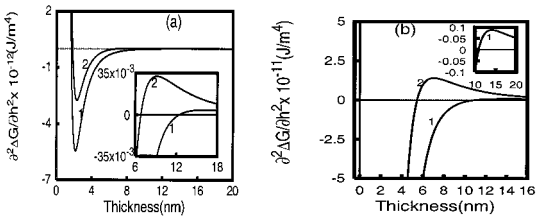

Figure 1. Variation of spinodal parameter for a model polystyrene film on an oxide-covered silicon wafer for (a) system I (high wettability) and (b) system II (low wettability). Qualitatively the lower part of the curves (not shown) in Figure 1b is similar to that shown in Figure 1a. Curve 1: heterogeneous patch. Curve 2: homogeneous substrate.

a combination of (a) a long-range van der Waals repulsion between a high-energy wettable substrate (for example, silicon) and the film, (b) an intermediate-range attraction, for example, between a low-energy, nonwettable thin coating of the substrate and the film, and (c) a very short-range repulsion close to the solid surface, for example, due to chain adsorption and compression and Born repulsion.[1,2,4,5,20,21,25] Qualitative variations of the second derivative of the excess free energy per unit area, $\partial^2\Delta G/\partial h^2 = \partial\phi/\partial h$, are as shown in Figure 1. The potential mimics the behavior of relatively low surface energy polymer films and of aqueous films on a majority of substrates, for example, silicon wafers, glass, and mica.[4,5,8] When the van der Waals component of the substrate surface tension exceeds that of the film material, long-range apolar van der Waals repulsion promotes the film stability and wetting.[4,5,20,21,23,24,43,44] The intermediate-range van der Waals attraction arises from a thin nonwettable coating of the substrate, for example, a low-energy oxide layer on the silicon substrate. The intermediate range attraction may also be due to non van der Waals forces arising from "hydrophobic attraction" in aqueous films and from entropic confinement effects for polymer films due to adsorbed/grafting at the solid−film interface.[43,44] One important class of such systems is the polymeric films on coated substrates, for example polystyrene films on an oxide (low-energy nonwettable) coated silicon (high-energy wettable) substrate.[2,6,8,10,16,17,23,24,29] The basic physics and relevance of thin films on homogeneously coated substrates have been addressed elsewhere.[23,24] The excess free energy per unit area, ΔG, and the conjoining pressure, ϕ, for a thin film on a coated substrate are obtained by a pairwise summation of various film−film, film−substrate, and film−coating van der Waals interactions.[43] A fairly general analytical representation of combined antagonistic (attractive/repulsive) long- and short-range intermolecular interactions (as in Figure 1) is given by

$$\Delta G = (S_s d_0^2 h^{-2})(R_{c2} + (R_{c1} - R_{c2})(1 + d_{c2}/h)^{-2} + (1 - R_{c1})(1 + d_{c1}/h + d_{c2}/h)^{-2}) + B_c/h^8 \quad (3)$$

where $R_{c1} = S_{c1}/S_s$ and $R_{c2} = S_{c2}/S_s$.

S_s and S_{c1} are the spreading coefficients of the film material on the substrate and the coating, respectively.[20,21,23,24] d_{c1} is the coating (e.g., oxide) thickness. The positive value of S_s signifies the long-range repulsion, whereas the negative coating−spreading coefficient represents an intermediate-range attraction. A still shorter-range repulsion may arise due to a chemically adsorbed or grafted layer of long branched polymer (connector) molecules ($S_{c2} > 0$ and d_{c2} are the spreading coefficient and the thickness of the adsorbed layer, respectively). Figure 1a shows the qualitative behavior of such a potential. Relatively thick films are spinodally stable ($\partial\phi/\partial h > 0$), and a window of spinodal instability (between two critical thicknesses, h_{C1} and h_{C2}[20]) exists at intermediate thicknesses. The analytical representation of the potential, eq 3, is for convenience, but the results presented here are valid for any potential of the type shown in Figure 1 regardless of the precise origin of the attractive/repulsive interactions.

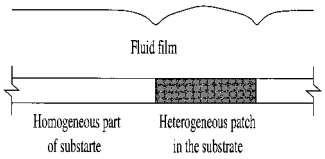

Figure 2. Schematic diagram of the thin film on a heterogeneous substrate.

The various thin film phenomena in heterogeneous systems are illustrated here with the help of a realistic set of parameters, while keeping contact, with a recent experimental study.[6,10,16] However, on the basis of a large number of simulations, we have verified that the essential physics and all of the qualitative observations are independent of the precise numerical value of the thin film potential. The following two distinct systems are chosen to illustrate the results.

System I (High Wettability). The homogeneous (bulk) system is characterized by the following parameters: $S_s = 20$ mJ/m^2, $S_{c1} = -12$ mJ/m^2, $S_{c2} = 2$ mJ/m^2, d_{c1} and d_{c2} are 2.5 nm and 1 nm, respectively. The equilibrium advancing contact angle is obtained from the extended Young−Dupre equation,[45−47] $\cos\theta = 1 + \Delta G(h_e)/\gamma$. This is small (=0.58°) for the homogeneous substrate. The ΔG versus thickness curve shows a minimum at 1.4 nm, which is close to the gyration-radius of a polymer used earlier.[6] The system has a higher critical thickness (h_{C2} where $\partial\phi/\partial h = 0$) of 6.85 nm; that is, films thicker than 6.85 nm are spinodally stable. To introduce heterogeneity, the nonwettable coating thickness on a small part of the substrate (patch) was varied from 2.5 to 4 nm, keeping other parameters the same. This increases the macroscopic equilibrium contact angle on the patch slightly to 1.7°. Variations of the spinodal parameter on the patch (curve 1 in Figure 1a) and on the surrounding homogeneous substrate (curve 2) are summarized in Figure 1a for this system. Figure 2 shows the schematic of the patch and its surroundings.

System II (Low Wettability). In the absence of chemical adsorption or grafting ($S_{c2} = d_{c2} = 0$; for simple liquids), a very steep Born repulsion, which arises due to the molecular orbit overlap, provides the necessary cutoff to prevent the divergence of van der Waals forces at film rupture.[25] Figure 1b shows such a potential. The homogeneous surroundings are characterized by the following parameters: $S_s = 20$ mJ/m^2, $S_{c1} = -8$ mJ/m^2, $d_{c1} = 2.0$ nm (curve 2 in Figure 1b). In contrast to the system I parameters given above, the absence of a soft repulsion increases the contact angle in this system to 37.5°. The system has a higher critical thickness of 5.5 nm in the characteristic curve of $\partial^2\Delta G/\partial h^2$ versus thickness of film (h). The heterogeneity was introduced by changing either

(43) Israelachvill, J. N. *Intermolecular and Surface Forces*; Academic Press: London, 1992.
(44) Van Oss, C. J.; Chaudhury, M. K.; Good, R. J. *Chem. Rev.* **1988**, *88*, 927.
(45) Brochard-Wyart, F.; di Meglio, J. M.; Quere, D.; de Gennes, P. G. *Langmuir* **1991**, *7*, 335.
(46) Sharma, A. *Langmuir* **1993**, *9*, 3580.
(47) Hirasaki, G. J. In *Contact Angel, Wettability and Adhesion*; Mittal, K. L., Ed.; VSP: Amsterdam, 1993; p 183.

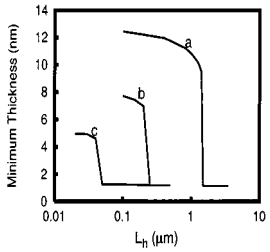

Figure 3. Dependence of indentation depth on the length scale of the heterogeneous patch, L_h, for films of thickness (a) 12.5 nm, (b) 8 nm, and (c) 5 nm. This figure as well as Figures 4−13 corresponds to system I. The heterogeneous patch and the surroundings are characterized by curves 1 and 2 of Figure 1a.

the coating thickness (d_{c1}) or the coating−spreading coefficient, S_c. For example, curve 1 of Figure 1b corresponds to a heterogeneous patch with $d_{c1} = 4$ nm.

2.3. Numerical Methods. The following nondimensional thin film equation,[4,5,23−25] obtained from its dimensional counterpart eq 1, governs the stability and spatiotemporal evolution of the film subjected to the excess intermolecular interactions (where $\Phi(H,X,Y) = [ho^3/(6|S_s|d_0^2)]\phi(x,y,t)$ and d_0 is the short-range cutoff thickness[44]).

$$\partial H/\partial T + \nabla\cdot[H^3\nabla(\nabla^2 H)] - \nabla\cdot[H^3\nabla\Phi] = 0 \qquad (4)$$

$H(X,Y,T)$ is the nondimensional local film thickness scaled with mean thickness h_0; X, Y coordinates are scaled with the characteristic length scale for the van der Waals case $(\gamma/(6|S_s|d_0^2))^{1/2}h_0^2$; and the nondimensional time T is scaled with $(\mu\gamma h_0^5)/(12S_s^2d_0^4)$.

We directly solved the 1-D and 2-D forms of eq 4 starting with an initial small amplitude volume preserving random perturbation, using central differencing in space with half node interpolation along with the Gear algorithm for time marching (especially suitable for the stiff equation). In what follows, the essential physics of the instability is illustrated with the help of 2-D simulations in Figures 3−13, and the complete 3-D morphological evolution is captured by 3-D simulations in Figures 14−29. To study the influence of the heterogeneity on the evolution, the linear stability analysis of eq 4 (based on the properties of the homogeneous surroundings) was carried out and the dominant spinodal length scale was computed.[4,5,23,24] The total length of the domain L was taken to be at least 3 times the value predicted by the above analysis. To address the problem of 3D-pattern selection, we used at least 80 × 80 grids for the full domain simulation ($L \times L$) using periodic boundary conditions.

3. Results and Discussion

3.1. Heterogeneous Patches and Edges: Critical Length Scales. Two simple models of chemical heterogeneity are considered: (a) a chemical step consisting of two semi-infinite planes filled with two different materials, which meet at a straight edge, and (b) a chemically distinct patch of finite extent surrounded by an infinite homogeneous surface. Case a can be thought of as a limit of case b when the patch size is very large.

The early stages of evolution obtained from simulations showed that the presence of a heterogeneity always creates a local depression regardless of whether the film is spinodally stable or unstable. Instability is induced at the patch boundary by flow in the direction of increasing wettability. The onset of local deformations is, however, not always sufficient to cause the film rupture and dewetting. Figure 3, based on 2-D simulations, shows the final (equilibrium) depth of the depression for increasing length scale (L_h) of the heterogeneous patch for three different film thicknesses of system I. The three cases considered (curves a−c) include all possible interesting combinations: (a) the thicker film of 12.5 nm is spinodally stable both on the surroundings and on a patch of any finite length; (b) the film of intermediate thickness (8 nm) is spinodally stable on the surroundings but unstable on a patch of length larger than its corresponding critical length scale, λ_c; (c) the thinner film of 5 nm thickness is spinodally unstable on the surroundings and also on a patch of length larger than its λ_c. These cases can be understood by an inspection of Figure 1a.

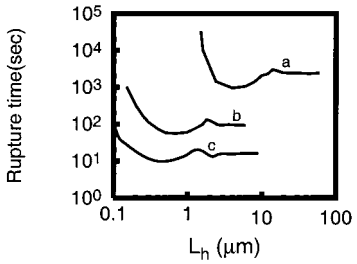

Figure 4. Dependence of rupture time, t_h, on the length scale of heterogeneity (patch), L_h, for films of different thickness: (a) 12.5 nm, (b) 8 nm, and (c) 5 nm.

Heterogeneity on extremely small lengths creates a local depression on the surface of the film but cannot induce rupture because of the stabilizing influence of the surface tension effect. An increase in the patch length causes a decrease in the magnitude of the surface tension restoring force and creates depressions of gradually increasing depth. Rupture occurs as the patch length exceeds a critical length, L_c. This critical length scale of the heterogeneity is at least 1 order of magnitude smaller than the spinodal length scale, even when the film is already spinodally unstable. For example, the spinodal length scale, λ_c, of a 5 nm thick film on the patch is 1.5 μm, but rupture can be induced by a patch as small as 0.05 μm (curve c of Figure 3). Films thicker than 6.85 nm, which are *spinodally stable* both on the surroundings and on the heterogeneous patch (of length less than λ_c), undergo deformation and rupture for larger lengths of heterogeneity (curves a and b of Figure 3). Thus, a heterogeneous patch of length larger than a critical L_c always causes rupture and dewetting. The spatiotemporal characteristics of the instability (e.g., morphology, rupture time, t_h, on a heterogeneous substrate) depend on the length of the heterogeneity. In the following section, we will discuss the influence of heterogeneity size on rupture time and on morphological pathways of evolution. The interfacial tension (γ) and viscosity (μ) of the polymer film have been taken to be 38 mJ/m^2 and 1 kg/(m s), respectively, for converting the results to typical dimensional values.

Figure 4 shows the dependence of rupture time on the length of a single heterogeneous patch, L_h. As the length of heterogeneity is increased beyond the critical length, the rupture time decreases rapidly to a minimum and then increases slightly before becoming independent of the length of the heterogeneity. As mentioned earlier, for very small lengths of the heterogeneity, the stabilizing influence of interfacial tension is very strong, since deformation also occurs on a short scale. Increasing the length of heterogeneity decreases this stabilizing force, thereby causing a decline in the rupture time (Figure 4). Beyond this point, the variation of rupture time shown in Figure 4 is best understood by examining the different pathways of evolution of instability that are shown in Figures 5−7 for increasing patch lengths. On a small patch,

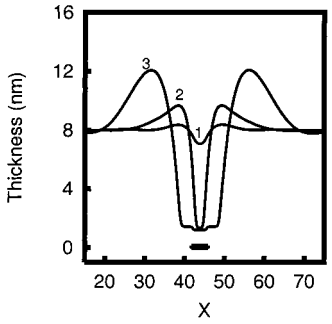

Figure 5. Evolution of surface instability in an 8 nm thin film on a substrate with a heterogeneous patch of 0.4 μm length at the center. Curves 1, 2, and 3 show the profiles at the following times: $t = 11$, 72, 144 s, respectively. The undisturbed part of the film has not been shown in this figure as well as in Figures 6 and 7.

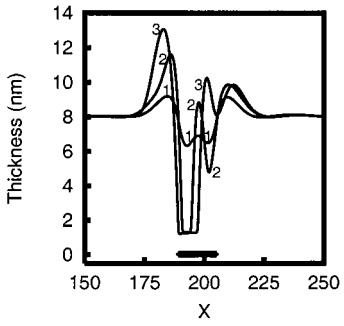

Figure 6. Evolution of surface instability in an 8 nm thin film on a substrate with a heterogeneous patch of 1.8 μm length at the center. Curves 1, 2, and 3 show the profiles at the following times: $t = 75$, 131, 143 s, respectively.

the outward flow induced at each of the patch boundaries acts in a cooperative manner, leading to the growth of a single depression which causes rupture at the *patch center* (Figure 5). Figure 5 depicts the evolution of a 8 nm thick film on a heterogeneous substrate, for a very small (0.4 μm) length of heterogeneity. Compared to the neutral spinodal length scale λ_c (4.366 μm) on the patch, the patch length is 1 order of magnitude smaller. Therefore, the film is spinodally stable both on the patch as well as on its surroundings. The film surface away from the hole remains undisturbed and flat at the time of rupture. The rupture time is 73.3 s (close to the minimum of curve b in Figure 4). The initial hole continues to grow across the patch boundary on the more wettable surroundings.

Beyond a certain length, a decreased cooperation of the patch boundaries in causing the outward flow, due to increased viscous resistance for outward flow, causes an increase in rupture time (right of the minimum of curve b of Figure 4). Thus, the minimum in the time of rupture in Figure 4 is due to a competing effect of surface tension and viscous flow. As the patch length increases, stabilization due to the surface tension decreases, but at the same time, the stabilizing influence of viscous flow increases because of the longer path for flow. The upturn in Figure 4 happens when the latter begins to dominate the former.

As the length of heterogeneity is further increased (1.8 μm; Figure 6), two nearly symmetric depressions form initially near the patch boundaries. As the depressions grow, both the viscous resistance for the film thinning and the surface tension stabilization become stronger. The central dimple diminishes and disappears. Eventually, only one of the depressions survives to grow to a full thickness hole, causing an *asymmetric, off-center rupture near one of the boundaries.* The time of rupture (132 s) at this point is a local maximum.

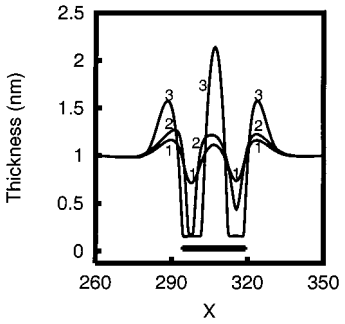

Figure 7. Evolution of surface instability in an 8 nm thin film on a substrate with a heterogeneous patch of 2.8 μm length at the center. Curves 1, 2, and 3 show the profiles at the following times: $t = 69$, 93, 105 s, respectively.

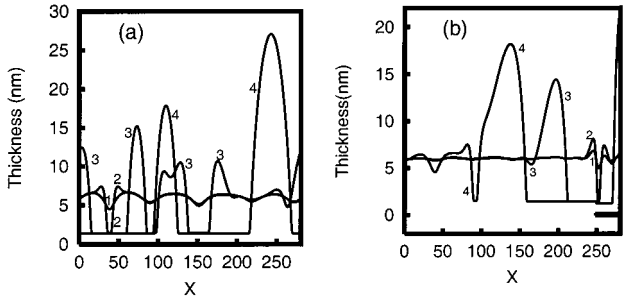

Figure 8. Evolution of surface instability in a 6 nm thick film. Part a shows evolution on a homogeneous substrate. Curves 1, 2, 3, and 4 show the profiles at the following times: $t = 1660$, 1736, 1982, 4 708 733 s, respectively. Part b shows evolution on a chemically heterogeneous substrate with a heterogeneous patch of 4 μm length in the right-hand corner. Curves 1, 2, 3, and 4 show the profiles at the following times: $t = 15$, 28, 589, 1793 s, respectively. The total simulation domain length is 36 μm ($\sim$5 times λ_m) for both parts a and b.

A further increase of length results in formation of two distinct holes separated by an intervening droplet, as in Figure 7. This is because the coupling between the flow induced by two boundaries becomes very weak and the surface tension stabilizing force becomes almost constant. The latter is due to the fact that the width of the depression at each boundary becomes constant and independent of the patch length. The rupture time now attains an asymptotic value (Figure 4). Thus, beyond a threshold length of the heterogeneity, L_T, the substrate having a patch may be considered to be analogous to a substrate having an edge, which divides two bulk regions of different wettabilities.

3.2. Other Features of Initial Evolution. The effect of heterogeneity is most clearly reflected in the morphology even during the early stage of evolution. Figures 5−7 have already shown the evolution of a stable film on a heterogeneous surface. Figure 8 summarizes and contrasts the initial evolution of an unstable film of 6 nm thickness on heterogeneous and homogeneous substrates. On a homogeneous surface, dewetting occurs by the formation of an undulating structure with a characteristic spinodal length scale, λ_m (Figure 8a). In contrast, on a heterogeneous substrate, a very rapid deformation of the film occurs near the boundary of the patch, leading to the formation of a localized hole, at which time the film surface away from the hole remains undisturbed and flat (Figure 8b). Asymmetric rims are formed around the hole. The time of rupture, t_h (28 s), is reduced by 2 orders of magnitude compared to the spinodal time, t_r (1736 s), by the presence of heterogeneity in this case. The surface undulations characteristic of a spinodal mechanism appear and evolve on the homogeneous surroundings at a much later time.

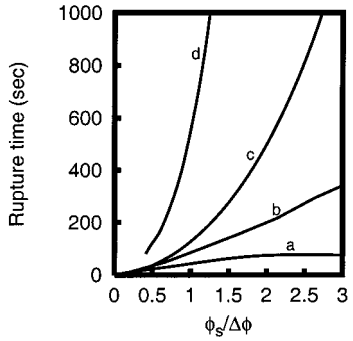

Figure 9. Dependence of rupture time, t_h, on the potential difference, $|\phi_s/\Delta\phi|$, on a substrate having a chemical step (heterogeneous edge) for films of different thickness: (a) 4 nm, (b) 6 nm, (c) 8 nm, and (d) 12.5 nm.

The ringlike hole expands to form a central drop on the patch and also a moving rim of increasing height on the patch surroundings. The far side of the rim where it meets the undisturbed film develops a slight depression (curve 3 in Figure 8b), as seen in experiments[27] and simulations.[25] The amplitude of this depression grows due to the spinodal mechanism, leading to the formation of a secondary hole (curve 4). This process of local ordering around a heterogeneously formed hole continues until the spinodal structures appear on the far away surroundings.

In general, when the first rupture occurs near the patch periphery in the form of a ringlike hole, both the inner and the outer contact lines retract to enlarge the dewetted area. The rate of retraction is higher on the less wettable part. In the extreme case of a completely wettable substrate, the contact line remains pinned at the boundary between the wettable and nonwettable parts. Similarly, the formation of layered secondary structures (seen in Figure 8b on the outside of the patch) can also occur on the patch if its dimension is much larger than the spinodal length scale of the patch. The mechanism of the formation of the layered structures both on the surroundings as well as on the patch is the same. These issues are illustrated later in greater detail with the help of 3-D simulations.

3.3. Effect of Wettability Gradient on Time Scale. In the presence of a strong wettability gradient, the characteristics of initial evolution on a heterogeneous substrate differ substantially from those expected for a spinodal process. A simple scaling analysis, ($f \sim \epsilon$, $\nabla^2 f \sim \epsilon/L^2$, $\nabla^2\Phi \sim \Delta\Phi/cL^2$, $c < 1$), of nondimensional form of eq 2 leads to the following characteristic time for the growth of instability.

$$T_h \sim 1/(-1/L^4 - (\partial\Phi/\partial H)/L^2 + \Delta\Phi/(\epsilon c L^2)) \qquad (5)$$

where $\Delta\Phi = |\Phi_s - \Phi_h|$ is the potential difference across the heterogeneous boundary evaluated at the mean thickness, L is the characteristic length scale of the instability, and ϵ is the amplitude of the depression.

$$T_h \sim 4[-(\partial\Phi/\partial H) + \Delta\Phi/\epsilon c]^{-2} \qquad (6)$$

Simulations reported in Figure 9 confirm the above dependence of the time of rupture on the potential difference, $|\Delta\phi/\phi_s|$. The simulations shown are for a chemical step having a heterogeneous edge. For thicker films that are spinodally *stable* on both the half planes on either side of the edge ($\partial\Phi/\partial H > 0$), the time of rupture shows a quadratic relationship with $|\phi_s/\Delta\phi|$ at large values of $\Delta\phi$ (curves c and d). For weaker wettability contrasts, the time of rupture climbs to infinity at some critical value of $|\phi_s/\Delta\phi|$, as predicted by eq 6. For spinodally unstable films ($\partial\Phi/\partial H < 0$) also, the dependence is quadratic for a very large value of $\Delta\phi$ ($|\phi_s/\Delta\phi| < 0.5$, curves a and b in Figure 9) and then becomes linear for intermediate values of $\Delta\phi$. At very low values of $\Delta\phi$, the slope of the curve decreases, and the time of rupture becomes almost constant and reaches the homogeneous spinodal time of rupture asymptotically (see inset in Figure 10).

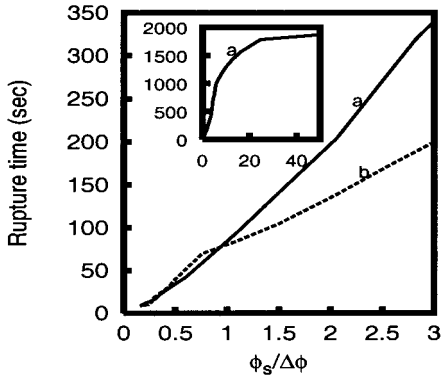

Figure 10. Comparison of the rupture time dependence on $|\phi_s/\Delta\phi|$ on substrates having a heterogeneous patch and a chemical step for a 6 nm thick film. The patch is of 1.2 μm length, on a 12 μm substrate. Curves a and b are for chemical step heterogeneity and a heterogeneous patch, respectively. The inset shows the rupture time dependence for the chemical step heterogeneity for very low values of the wettability contrast, $\Delta\phi$.

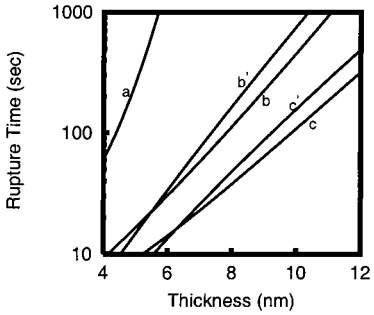

Figure 11. Variation of the rupture time with film thickness. Curve a: homogeneous substrate (Figure 1a, curve 2). Curves b, c and b′, c′: heterogeneous substrate with a chemical step (edge) obtained from solution of the exact nonlinear and linearized equations, respectively. Wettability contrast is increased from curve b (coating thickness is increased in a step from 2.5 to 4 nm (Figure 1a)) to curve c (coating thickness is increased in a step from 2.5 to 6 nm).

Figure 10 compares the rupture times on a finite patch and on a heterogeneous step. It clearly indicates that a cooperative effect of the two boundaries of the patch in causing the flow reduces the rupture time (unless the patch length is very small, in which case the surface tension stabilization is important, e.g., Figure 4). As discussed in Figure 4, even a small patch behaves much like a heterogeneous step when $\Delta\phi$ is large, and the time of rupture becomes independent of the patch size.

Figure 11 compares the times of rupture from the heterogeneous mechanism and from the spinodal mechanism, both determined on the basis of simulations. The total length of heterogeneity has been taken to be greater than L_T. An increased wettability contrast (curves a−c) decreases the time of rupture and also decreases the exponent for its dependence on the film thickness. Thus, the difference between the heterogeneous and the spinodal times increases for thicker films, and the role of heterogeneity becomes more important for the thicker films. Figure 11 also compares the rupture time obtained from

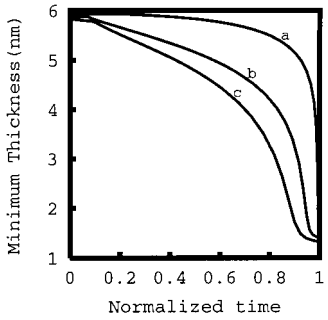

Figure 12. Evolution of minimum thickness in a 6 nm thin film with normalized time for homogeneous (curve a) and different heterogeneous systems (curves b and c) with increasing wettability contrast from curve b to curve c. The time is normalized on the basis of rupture times of 2225, 93, and 20 s, for curves a, b, and c, respectively.

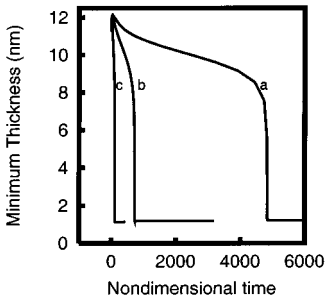

Figure 13. Evolution of minimum thickness in a 12.5 nm stable film with time for different heterogeneous systems with increasing wettability contrast from curve a to curve c. For curves a, b, and c the values of $|\Delta\phi/\phi_s|$ are 0.41, 0.59, and 1.11, respectively.

the nonlinear (eq 4) and the linear simulations (eq 2). A good semiquantitative match shows that the linearized equation can be used as a first approximation for assessing the role of heterogeneity in reducing the time of rupture. The linear theory overpredicts the time of rupture for relatively thick spinodally stable films because the stabilizing influence of the spinodal term is overestimated by evaluating Φ_H at the initial (mean) thickness.

3.4. Kinetics of Initial Evolution until Rupture. The effect of heterogeneity is also clearly reflected in the dynamics of initial stages of evolution of thinner (unstable) films, as shown in Figure 12 for a spinodally unstable film. This figure compares the evolution of the minimum film thickness on a homogeneous substrate (curve a) and on heterogeneous substrates of different wettability gradients ($|\Delta\phi/\phi_s| = 0.923\,18$ for curve b and $|\Delta\phi/\phi_s| = 2.823$ for curve c). Time is normalized by the corresponding rupture time in each case to clearly show the differing characteristics of the growth. For films on homogeneous substrates, the spinodal theory predicts a slow exponential growth of surface instability initially. An explosive nonlinear phase of growth occurs at late times just before rupture (curve a). In contrast, the growth of instability on heterogeneous surfaces becomes increasingly uniform over time with increased wettability contrast (curves b and c). The nonlinear spinodal effect comes into play at the last stage of evolution and accelerates the growth further.

Figure 13 shows the evolution of minimum thickness in a thick spinodally *stable* film for different wettability contrasts. After a short initial transient, the minimum thickness declines almost linearly with time, until a very fast final phase of very short duration ruptures the film.

3.5. 3-D Morphological Patterns Induced by a Heterogeneous Edge. Figure 14 shows the key morphological features of the evolution of a thin film on a heterogeneous step as obtained from a nonlinear 3-D simulation for a 5 nm thick, spinodally unstable film. The upper half-space in this simulation is less wettable than the lower half. In all of the gray scale figures, we have used a continuous gray scale to denote thickness, with increasingly darker shades for thicker regions. The flow induced by the heterogeneity initially causes a rapid decline in the local thickness along the edge. Dewetting is initiated by the formation of several primary depressions, which coalesce to form a straight edge. The rim adjacent to the contact line has greater elevation on the more wettable part, and its retraction is also slower. The far side of the retracting rim on the less wettable part develops a depression, as is discussed clearly in Figure 8. The growth of this local valley is assisted by the spinodal mechanism (intermediate range attraction), which in turn engenders a new generation of slightly elliptical holes that are lined up along the far side of the rim. Retraction of the primary rim stops with the coalescence of holes. A new retracting edge is formed, and the process repeats over until the uniform spinodal structures start appearing on the substrate. Eventually, the long liquid ridges formed also fragment into droplets due to the Rayleigh instability of cylindrical threads. The mean spacing (parallel to the edge) between the primary, as well as the secondary, holes/depressions is of the same order of magnitude as the spinodal length scale, λ_m, corresponding to the less wettable region. Thus, dewetting initiated by a heterogeneous edge engenders a variety of locally ordered patterns that are lined up in the direction of the edge, for example, a string of holes and liquid ridges and a string of droplets, at different stages of evolution. Since the process of local ordering in unstable films stops after the formation of spinodal structures, the local ordering is longer ranged when the heterogeneous and the spinodal time scales are vastly different, for example, for thicker films and higher wettability contrasts. Thus, the interlayer spacing between the ordered structures (in the direction normal to the heterogeneous edge) increases with an increased difference between the spinodal and heterogeneous time scales (as in the simulations shown later for heterogeneous patches). For this reason, the layering of secondary structures is greatly delayed on the more wettable part of the substrate in Figure 14.

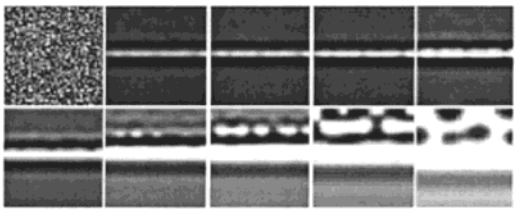

Figure 14. Morphological evolution in a 5 nm thick film on a heterogeneous step. The upper half of the substrate is less wettable than the lower half. In this image, as well as in the subsequent images, a continuous gray scale between the minimum and the maximum thickness in each picture has been used. Gray scale pictures in the two rows correspond to (from left to right) T (nondimensional time) = 0, 228, 258, 281, 329, 376, 539, 727, 1111, and 2106, respectively. The area of each cell is $22\lambda_m^2$ ($10 \times 10\ \mu m^2$), based on the less wettable part (curve 1 of Figure 1a). The potentials of the chemical step for this figure as well as for Figures 15 and 16 correspond to curves 1 and 2 of Figure 1a.

Ordered structures, however, cannot form during heterogeneous dewetting when the film is spinodally stable on either side of the heterogeneous edge, as shown in Figure 15. Figure 15 summarizes the evolution of a spinodally stable, 12.5 nm thick film. The initial growth

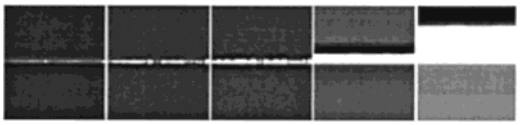

Figure 15. Morphological evolution in a spinodally stable 12.5 nm thick film (Figure 1a) on a heterogeneous step. The upper half of the substrate is less wettable than the lower half. Gray scale pictures from left to right correspond to $T = 526, 637, 747, 2155$, and 20 933, respectively. The area of each cell is 150 × 150 μm^2.

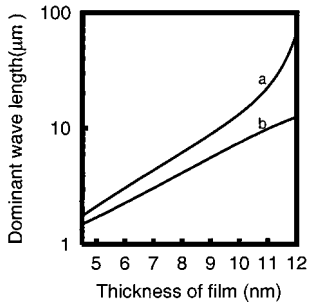

Figure 16. Variation of length scale of instability with thickness of film: curve a, spinodal length scale on a homogeneous substrate (Figure 2a, curve 1); curve b, length scale on a heterogeneous substrate with a chemical step.

of instability again occurs by the flow normal to the edge induced by the heterogeneity, which leads to the film rupture by the formation of a string of holes as the minimum thickness enters the spinodally unstable regime. Coalescence of holes results in a straight contact line, which retracts more rapidly on the less wettable side of the heterogeneous edge. However, the formation of secondary structures ahead of the moving rim is now suppressed, since the undisturbed film is spinodally stable. A slight depression formed at the far side of the moving rim in this case cannot grow.

Figure 16 (curve b) shows the mean spacing between the primary holes/depressions formed along the edge of heterogeneity before the onset of dewetting in spinodally unstable films. Curve a in the same figure compares the spinodal length scale (evaluated at the mean thickness) on the less wettable part, λ_m. A somewhat smaller mean spacing is obtained in "nucleated" holes, since they form at some lower effective thickness, that is, from a valley that is already formed initially by the more rapid heterogeneous flow. The thickness dependence of the mean hole spacing on the heterogeneous edge ($\lambda \propto h^{2.27}$ for $h <$ 12 nm) is, however, very similar to that of the spinodal length scale ($\lambda_m \propto h^{2.24}$ for $h < 9$ nm). A greater divergence from the spinodal length scale results as the spinodally stable boundary ($h > 12$ nm; $\lambda_m \rightarrow \infty$) is approached. This is again because holes/depressions form at a lower thickness, resulting in a finite mean spacing even as the spinodal length scale evaluated at the mean thickness diverges ($\lambda_m \rightarrow \infty$).

3.6. 3-D Morphological Patterns on Finite Heterogeneities. 3-D nonlinear simulations on substrates containing finite heterogeneous patches provide additional novel morphological features that can be directly compared with experiments. The most prominent of these readily identifiable features are discussed below.

3.6.1. Morphological Features in Relatively Thin Films: Castle-Moat Structure, Concentrically Arranged Droplets, and Ripples. The coexistence of undulations, drops, and holes at the initial stage of dewetting is one of the important effects of heterogeneity on the pattern formation. Such mixed morphologies can

Figure 17. Morphological evolution in a 3 nm thick film on a homogeneous substrate (curve 2 of Figure 1a) of area 59λ_m^2 (10 × 10 μm^2). The pictures from left to right correspond to T = 0.005, 4160, 11 489, 26 157, and 47 345.

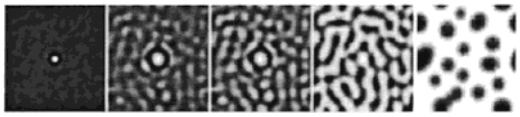

Figure 18. Morphological evolution in a 3 nm thick film on a substrate with a centrally located heterogeneous patch of length 0.5 μm (0.5 times λ_m of patch). The area of the domain is 59λ_m^2 (10 × 10 μm^2), based on the more wettable surroundings. The pictures from left to right correspond to T = 572, 4930, 6114, 10 923, and 47 017. For this picture as well as for figures 19, 22, 23, 25, 26, 28, and 29, the heterogeneous patch and surroundings are characterized by the potentials shown in curves 1 and 2 of Figure 1a, respectively.

result for different film thicknesses under different characteristics of the patch. The important characteristics of the heterogeneous substrate are the length scale of the heterogeneity and the potential gradient it produces. To clearly contrast the results, the characteristic morphologies of dewetting on *homogeneous* substrates are first summarized:[4,5,48] (a) relatively thin films to the left of the minimum in the spinodal parameter dewet directly by the formation of droplets, (b) intermediate thickness films break up by the formation of a transition bicontinuous structure made up of long hills and valleys, and (c) relatively thick films dewet by the formation of isolated circular holes. Some recent studies have indeed shown a shift in the morphological evolution from droplets to holes as the film thickness increases[2,6] and also when the spinodal minimum shifts to higher thickness by changing the substrate properties.[49]

The major events in the evolution of the spinodal pattern on a homogeneous substrate for an intermediate thickness of 3 nm are summarized in Figure 17. The film thickness in this case is close (slightly right) to the minimum in the spinodal parameter, $\partial^2\Delta G/\partial h^2$ of the homogeneous substrate (Figure 1a). As expected from the linear theory, the initial random disturbances first reorganize into a small-amplitude structure on the dominant length scale, λ_m. The ridges broaden and increase in height due to the coalescence of depressions and flow from the valleys. Finally, fragmentation of uneven long ridges directly produces an array of microdroplets.

In contrast to the case in Figure 17, evolution of a 3 nm thick film on various heterogeneous substrates shows coexistence of mixed morphological features following the film rupture, for example, holes and surrounding spinodal undulations (Figure 18) and holes, drops, and undulations (Figures 19 and 20). Figures 18−20 depict several distinct pathways of dewetting on substrates with different characteristics of the heterogeneity. Evolution is shown over an area of (10 × 10) μm^2. Figure 18 summarizes the time evolution on a substrate with a small less wettable patch of area (0.5 × 0.5) μm^2. The patch size is smaller than the spinodal length scale, λ_m (0.95 μm), of the patch. A lone expanding hole first forms at the patch center and grows across the patch boundary. At the onset of dewetting,

(48) Singh, J.; Sharma, A. *J. Adhesion Sci. Technol.* **2000**, *14*, 145.
(49) Maas, J. H.; Cohen Stuart, M. A.; Leermakers, F. A. M.; Besseling, N. A. M. *Langmuir* **2000**, *16*, 3478.

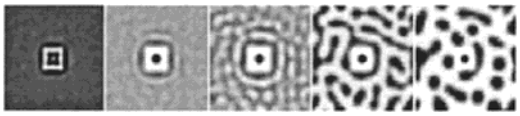

Figure 19. Morphological evolution in a 3 nm thick film on a substrate with a centrally located moderately large patch of length 2 μm (2 times λ_m of patch). The pictures from left to right correspond to T = 908, 3232, 6177, 15 001, and 27 067. The area of each cell is $59\lambda_m^2$ (10×10 μm^2).

Figure 20. Morphological evolution in a 3 nm thick film with a centrally located *more wettable patch* of length 2 μm (1.5 times λ_m of patch). The patch and the surroundings of this figure as well as of Figure 24 are characterized by the potential shown in curves 2 and 1 of Figure 1a, respectively. The pictures from left to right correspond to T = 689, 1404, 2053, 4145, and 6567. The area of each cell is $110\lambda_m^2$ (10×10 μm^2), based on the less wettable surroundings.

much of the film away from the hole remains undisturbed. For this relatively thin film, the twin processes of spinodal growth on the surroundings and local ordering around the hole rim appear at about the same time. Further growth of the hole is now arrested, and its rim and spinodal structures elsewhere all undergo fragmentation into droplets due to the Rayleigh instability. Droplets become increasingly circular due to surface tension. The initial signature of the heterogeneity is rather completely obliterated after a long time.

Figure 19 shows the time evolution on a substrate containing a bigger, less wettable patch of (2×2) μm^2 area. Dewetting now occurs through the formation of several holes at the edge of the patch, as in the case of a heterogeneous step. Coalescence of holes traps a droplet at the patch center, leading to the castle-moat morphology. As in the earlier case, the evolution proceeds by the appearance of local ordering around the hole-rim and spinodal features on the surroundings. The novel morphological feature in all cases of a moderately large less wettable patch are the onset of dewetting at the patch periphery leading to the formation of a "castle-moat" pattern. Mixed morphologies consisting of apparently nongrowing holes in combination with undulations, as well as ringlike holes with central droplets, have been experimentally observed.[7,15]

What happens when the heterogeneity is *more* wettable than its surroundings? This question is addressed in Figure 20, where rupture is again caused at the patch periphery by the flow of liquid *toward* the patch center rather than away from it. In all such cases, a castle-moat pattern results regardless of the patch dimensions, as long as it is larger than a critical size necessary to induce dewetting.

Figure 21 characterizes the shift in morphology as the film gets thicker and/or the patch size further increases. In this figure, a 3.5 nm thick film rests on a heterogeneity of 7 μm diameter, almost 5.4 times the λ_m (1.3 μm) on the patch. The primary instability and dewetting in this case are again initiated by the formation of a ringlike depression at the patch boundary. However, the secondary local ordering in this case can proceed both within and outside the patch boundaries, giving the appearance of a more complex, "ripple"-like structure. This ripple-like pattern bears a striking resemblance to the pattern observed by Guerra et al.[14] At later times, spinodal undulations also cover the surroundings away from the site of local ordering,

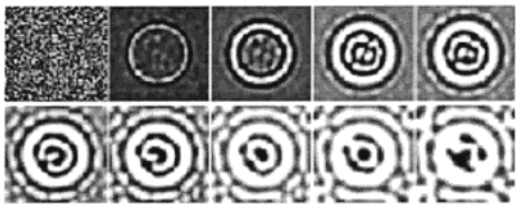

Figure 21. Morphological "ripple"-like pattern evolution in a 3.5 nm thick film on a substrate with a centrally located large, less wettable patch of diameter 7.2 μm. The wettability contrast is reduced by changing the coating thickness of the patch to 3.25 nm. The surrounding is characterized by the potential shown in curve 2 of Figure 1a. The area of each cell is $59\lambda_m^2$ (12×12 μm^2), based on the surroundings. The pictures in the two rows correspond to (left to right) T = 0.0065, 402, 1285, 2526, 3098, 4434, 5270, 6453, 9114, and 11 473.

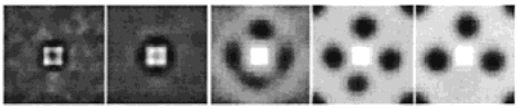

Figure 22. Morphological evolution in a 2 nm thick film on a substrate with a centrally located, less wettable patch of length 0.6 μm (0.8 times λ_m of patch). The pictures from left to right are at T = 549, 2978, 71 062, 135 643, and 322 275. The area of each cell is $5.5\lambda_m^2$ (3×3 μm^2), based on the surroundings.

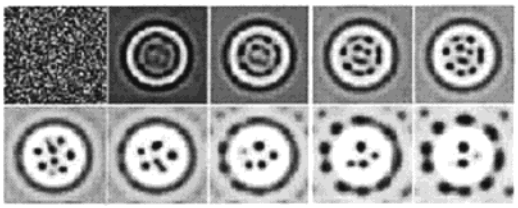

Figure 23. Morphological evolution in a 2 nm thick film on a substrate with a large, centrally located, less wettable circular patch of diameter 3.6 μm (4.7 times λ_m of patch). The area of each cell is $22\lambda_m^2$ (6×6 μm^2), based on the surroundings. The pictures in the two rows (from left to right) correspond to T = 0.035, 9225, 15 609, 18 539, 22 171, 26 935, 44 865, 67 176, 98 729, 145 034, and 176 996.

and the whole structure begins to disintegrate into droplets. As discussed earlier, the number of ripples or ordered alternating layers depends on the characteristics of the heterogeneous patch and the film thickness.

The above pathways of dewetting and associated morphologies are characteristic of films in a range of thickness where dewetting occurs by the formation of a bicontinuous pattern on homogeneous substrates. Figures 22−24 depict the time evolution of a thinner film, which is to the left of the minimum in the spinodal parameter in Figure 1a. Spinodal dewetting on a homogeneous surface in this case occurs directly by the formation of largely circular droplets rather than by long undulations. A small less wettable heterogeneity again causes dewetting by a localized hole, but its rim now directly disintegrates into circular droplets arranged on a square lattice around the central hole. At still later times, ripening reduces the number of droplets. A larger less wettable patch gives rise to the more complex and longer-range ordering, an example of which is shown in Figure 23. Initially, dewetting occurs at the periphery of the patch, resulting in a ringlike depression flanked by an inner and an outer rim. The inner rim on the patch disintegrates directly into circular droplets arranged on the periphery of the patch. On large patches, some ordering also occurs in the interior of the patch, which also produces droplets. While the process of droplet ripening continues on the patch, the outer rim also breaks up to form droplets

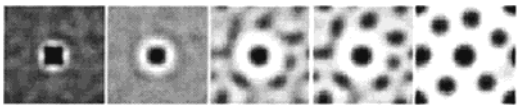

Figure 24. Morphological evolution in a 2 nm thick film with a centrally located *more wettable patch* of length 0.6 μm (0.47 times λ_m of patch). The pictures from left to right correspond to $T = 1565$, 5616, 19 159, 23 428, and 59 381. The area of each cell is $15.5\lambda_m^2$ (3×3 μm^2), based on the less wettable surroundings.

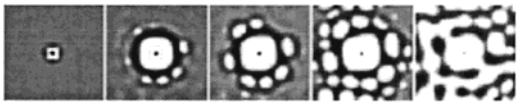

Figure 25. Morphological *ordered* pattern evolution in a 5 nm thick film on a substrate with a centrally located, less wettable patch of 2 μm ($\sim\lambda_m$ of patch). The area of each cell is $29.4\lambda_m^2$ (20×20 μm^2), based on the surroundings. The pictures from left to right correspond to $T = 336$, 4077, 4934, 8804, and 6331.

arranged on a larger circle. The same process of pattern ordering can continue on even larger scales (as seen in the last three pictures in Figure 23) until the appearance of spinodal features on the surroundings.

Figure 24 shows that similar patterns result even when the patch is *more* wettable than the surroundings. The instability on a small patch in such a case leads to a concentric pattern of droplets surrounding a central drop, rather than a hole, as in Figure 22.

Arrangements shown in Figures 23 and 24 are similar to experimentally observed columns "nucleated" in thin polymer films by the application of an electric field.[50] A small heterogeneity in the system, possibly of local electric field, was observed to lead to a concentric arrangement of columnar droplets rather than the hexagonal packing obtained by the spinodal mechanism.[50]

3.6.2. Morphological Features in Relatively Thick Films: Concentric Arrangement of Holes. On homogeneous substrates, films thicker than a certain critical thickness to the right of the spinodal minimum break up and dewet by the formation of largely circular holes.[4,5] Figure 25 summarizes the evolution of a relatively thick film (5 nm) on a substrate containing a less wettable heterogeneous patch. The initial rupture occurs rapidly by the formation of a rapidly expanding hole, as in the case of thinner films. At later times, the spinodal instability preferentially engenders slightly elliptical secondary holes surrounding the far side of the rim where a slight depression forms initially. A repeated layering of holes continues to occur until the spinodal holes start to appear on the homogeneous surroundings. Such an ordered structure has also been reported for semicrystalline polymer PCL on a glass surface during spin coating.[11] At later times, hole coalescence engenders circular uneven liquid threads, which have the tendency to break up into droplets (last picture of Figure 25). To show the effect of film thickness on ordering phenomena and the hole size distribution, the time evolution of a slightly thicker film (5.5 nm) on an identical substrate is shown in Figure 26. An increase in the film thickness increases the spinodal time more than the heterogeneous time of rupture. Therefore, the heterogeneously nucleated hole grows to a larger size before secondary holes start to appear at its periphery. Thus, on a substrate containing many heterogeneous sites, diameter of heterogeneous holes increases compared to the spinodal holes at higher film

(50) Schaffer, E.; Thurn-Albrecht, T.; Russel, T. P.; Steiner, U. *Nature* **2000**, *403*, 874.

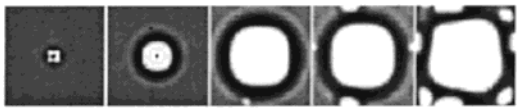

Figure 26. Evolution in a 5.5 nm thick film on a substrate identical to that in Figure 25 showing the effect of thickness on ordered pattern formation. The pictures from left to right correspond to $T = 258$, 2095, 6424, 7162, and 9076.

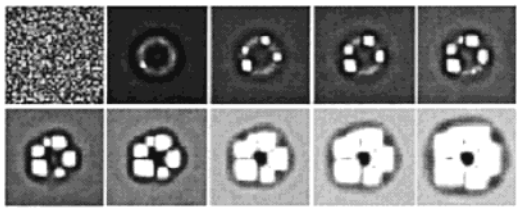

Figure 27. Morphological "flower"-like pattern evolution in a 2 nm thick film on a heterogeneous substrate with a centrally located, more wettable circular patch of diameter 0.4 μm (2 times λ_m of patch). The area of each cell is $19.5\lambda_m^2$ (1×1 μm^2). The pictures in the two rows from left to right correspond to $T = 0$, 42, 44.4, 46, 47, 49, 51, 59, 65, and 74. The patch and surroundings are characterized by the potentials shown in curves 1 and 2 of Figure 1b, respectively.

thicknesses, since heterogeneously formed holes can grow to a much bigger size before the appearance of the spinodal holes. Also, the relative number density of spinodal holes decreases with increased thickness since a larger substrate area is covered by the heterogeneous holes. Both of these conclusions are supported by the experiments of Thiele *et al.*[9] which indeed show an increase in the diameter of larger (heterogeneous) holes and a decrease in the number density of smaller (spinodal) holes in evaporating water films at lower rates of evaporation. This is expected, since a decrease in the rate of evaporation causes the film rupture by the spinodal mechanism at higher mean thickness.

Figure 27 shows the evolution of an interesting flower-like structure, which forms around a sufficiently large less wettable heterogeneity where rupture occurs by the formation of several holes around the patch periphery. In this particular simulation, the holes grow faster toward the patch center, since the wettability of the patch is lower. Growth of holes *before their eventual coalescence* forms "petals" arranged around a pool of liquid trapped near the patch center. Depending on the area of the patch, multilayers of such flower-like patterns can also be obtained as intermediate stages of evolution. The formation of a flower-like structure therefore always occurs as long as the rupture is initiated at the patch boundary by several holes, no additional spinodal features appear within the patch, and the spinodal features outside the patch evolve at a much later time. Clearly, persistence of a flower-like arrangement is encouraged by slower growth and delayed coalescence of the secondary holes. Thus, factors such as higher film viscosity and elasticity in higher molecular weight films should increase the lifetime of a "flower".

3.6.3. Rupture of Spinodally Stable Films. As mentioned earlier, one of the important effects of chemical heterogeneity is that it can induce rupture even of a spinodally stable film if the initial heterogeneity-driven flow can locally lower the thickness sufficiently so that spinodal instability can become operative. Figure 28 shows the formation and growth of a lone hole in a relatively thick film (10 nm) which is spinodally stable both on the surroundings and on the patch (since the patch size, 4 μm, is much smaller than $\lambda_m \approx 12\,\mu$m). The spinodal waves

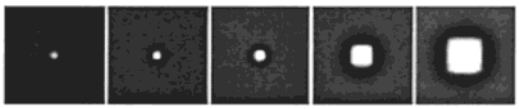

Figure 28. Evolution in a 10 nm thick film on a heterogeneous substrate with a circular patch of 4 μm (0.3 times λ_m of patch). The area of each cell is 40 × 40 μm^2. The film is spinodally stable both on the patch and on the surroundings. The pictures from left to right correspond to T = 84, 95, 125, 746, and 1866.

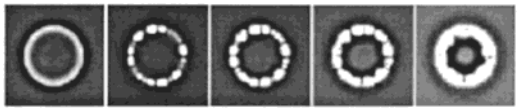

Figure 29. Evolution in a 10 nm thick film on a heterogeneous substrate with a circular patch of 24 μm (~2 times λ_m of patch). The area of each cell is 40 × 40 μm^2. The film is spinodally stable on the surroundings. The pictures from left to right correspond to T = 75, 268, 283, 300, and 352.

remain absent at all times, and the film away from the growing hole remains flat. No additional secondary morphological features appear even as the hole rim continues to build. This mode of dewetting is similar to that observed by Stange et al.[10] for relatively thick polystyrene films on a SiO_2-coated Si surface.

Additional morphological features can however appear on a large patch where rupture occurs by the formation of several holes at the periphery rather than a single hole centered on the patch. Such a possibility is shown in Figure 29. Intermediate stages of evolution can produce an interesting flower-like structure, which, as shown earlier, is a somewhat generic feature of the systems where rupture occurs at the patch periphery by several holes, which do not coalesce rapidly.

4. Conclusions

This study shows that the presence of chemical heterogeneities on very small length scales, substantially smaller than the spinodal length scales, can destabilize and rupture a thin film by engendering a gradient of chemical potential along the solid−liquid interface. The heterogeneous dewetting is possible even for very small and experimentally difficult to resolve macroscale wettability contrasts, for example, for differences in contact angles as small as 1°. The stronger flow in this heterogeneous-nucleation mechanism is derived from a spatially fixed microscale wettability contrast rather than from temporally evolving local variations in the film thickness. The latter is associated with the spinodal instability on homogeneous substrates. Thus, even a spinodally stable film can undergo rupture if the local thickness is initially reduced by the heterogeneous mechanism to a point where the spinodal condition is satisfied, and the two mechanisms achieve a cooperative effect thereafter. The time scale can be many orders of magnitude smaller than the spinodal time scale and shows a weaker dependence on the film thickness as compared to that of the spinodal time scale. Thus, the heterogeneous mechanism becomes most prominent for relatively thick films. For unstable films, the number density of holes along a heterogeneous edge does not differ appreciably from that predicted from the spinodal mechanism. However, the discrepancy increases near and beyond the critical thickness, since the spinodal length scale becomes infinite, whereas the distance between heterogeneously produced holes remains finite. The dynamics of initial evolution and morphological features contain the following clear-cut signature of the presence of heterogeneities: (a) the absence of surface waves preceding rupture of the film, (b) mixed or distinct morphologies on different parts of the substrate, (c) a "castle-moat" pattern where a central drop is surrounded by a ringlike depression or a full thickness hole, and (d) local ordering of the structure inside and outside the patch. The relationship between the morphological pattern and the characteristics of the heterogeneities has been studied. It is hoped this study will aid in accessing the role of heterogeneities in thin film experiments where many of the above features are frequently witnessed and will also help in the design of thin film experiments on chemically patterned substrates.

Acknowledgment. Discussions with G. Reiter, S. Herminghaus, U. Steiner, A. Karim, and R. Khanna are gratefully acknowledged. This work was supported by a grant from the Indo-French Center for the Promotion of Advanced Research.

LA000759O